Supplementary Materials S1

Supplementary Materials Table S1. Observation wells, Kamchatka Peninsula

Well	Coordinates	Depth, m Open interval, m	Lithology: age, composition	Discharge rate, q, dm^3/s; Water-level depth, h, m	Water temperature, °C	Water mineralization, g/dm^3	Water type	Gas composition	Observations: covered period, frequency of measurements
GK-1	53.28°N 158.40°E	1261 400–1261	Q, N, K_2, tuff, siltstone, shale	flowing, q=0.1	16	10	Cl–Na–Ca	free gas, CH_4–N_2	1986–1998, 3 days
M-1	53.18°N 158.28°E	600 310–313 407–410 553–556	N, tuff	flowing, q=1.5	16	0.25	SO_4–Ca–Na	dissolved gas, N_2	
G-1	53.05°N 158.66°E	2500 1710–1719 1750–1754 1790–1799 2415–2424	Q, K_2, diorite, shale	flowing, q<0.001	10	12	Cl–Na	free gas, CH_4–N_2	
E-1	53.26°N 158.48°E	665 625–645	N, tuff	piezometric well, h=28	10	1.5	Cl–HCO_3–Na	free gas, N_2–CH_4	1987–2016: 03.01.1987–08.07.1994, 1 day; 29.01.1996–2016, 5–10 minutes
YuZ-5	53.17°N 158.41°E	800 310–800	K_2, mudstone, shale	piezometric well, h=1.5	14	0.45	HCO_3–SO_4–Na–Ca	dissolved gas, N_2	09.09.1997–2016, 5–10 minutes

A

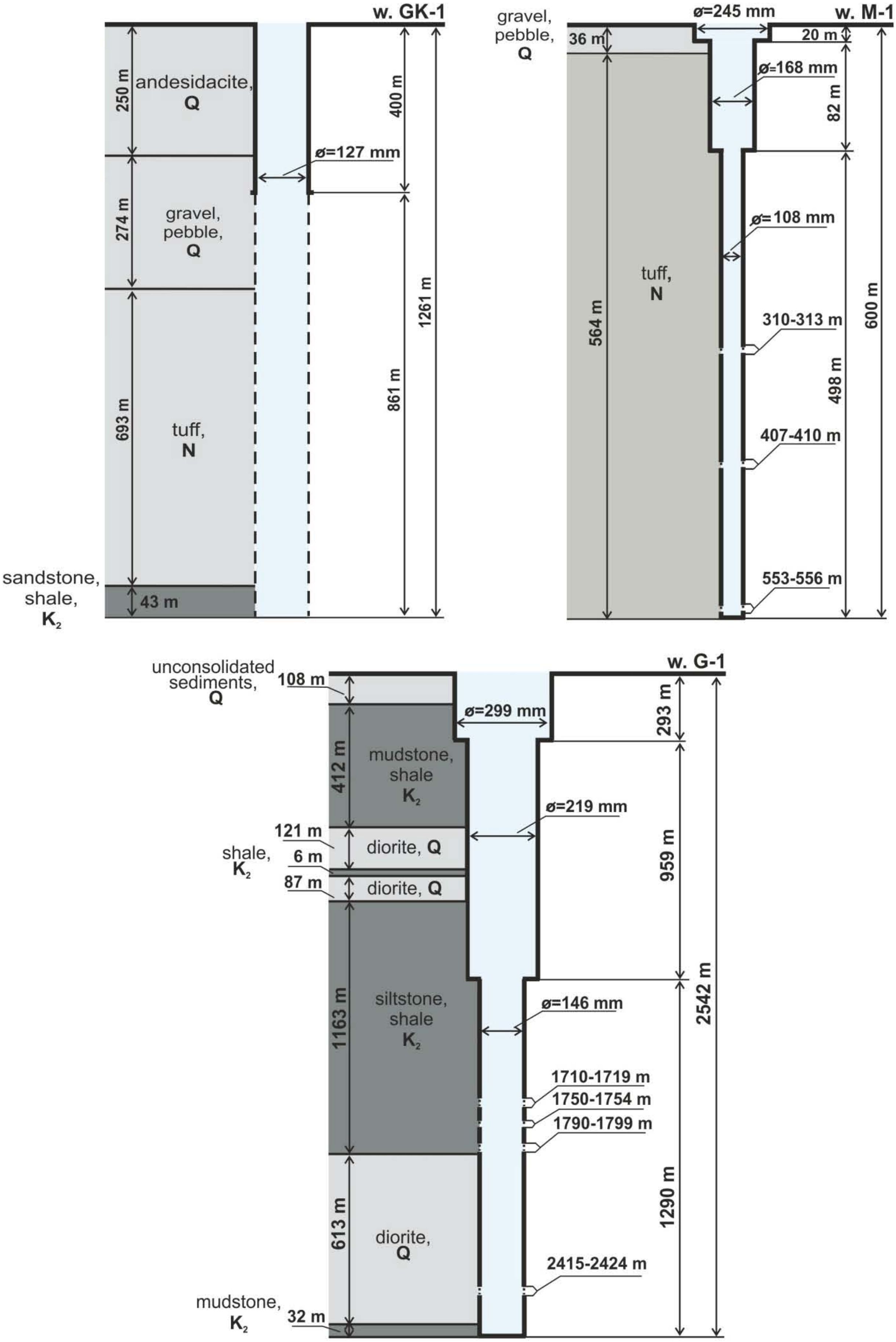

w. GK-1
andesidacite,
Q
250 m
400 m
ø=127 mm
gravel,
pebble,
Q
274 m
tuff,
N
693 m
861 m
1261 m
sandstone,
shale,
K2
43 m
w. M-1
gravel,
pebble,
Q
36 m
ø=245 mm
20 m
ø=168 mm
82 m
ø=108 mm
tuff,
N
564 m
310-313 m
407-410 m
553-556 m
498 m
600 m
w. G-1
unconsolidated
sediments,
Q
108 m
ø=299 mm
293 m
mudstone,
shale
K2
412 m
ø=219 mm
121 m
diorite, Q
shale,
K2
6 m
87 m
diorite, Q
959 m
siltstone,
shale
K2
1163 m
ø=146 mm
1710-1719 m
1750-1754 m
1790-1799 m
2542 m
diorite,
Q
613 m
1290 m
2415-2424 m
mudstone,
K2
32 m

B

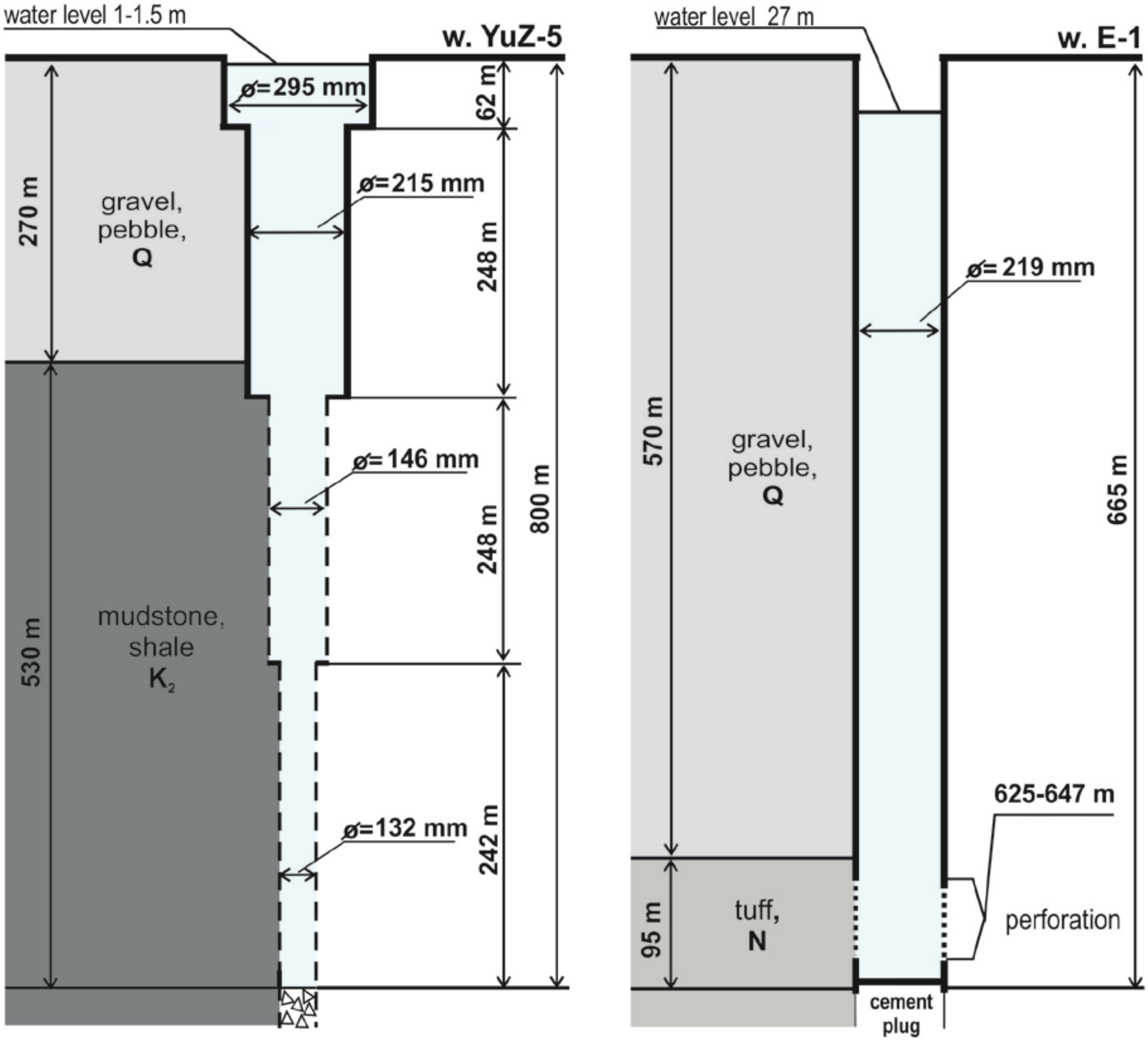

Supplementary Materials Figure S1. Structure of observation wells, Kamchatka Peninsula: **(A)** – flowing wells: GK-1, M-1, G-1; **(B)** – piezometric wells: YuZ-5, E-1.

Supplementary Materials Table S2. Earthquakes (https://earthquake.usgs.gov/earthquakes/, http://sdis.emsd.ru/info/earthquakes/catalogue.php) preceded by hydrogeological precursors in at least two observation wells, Kamchatka Peninsula

No	**Date,** dd.mm.yyyy	**Earthquake epicenter**	**Depth** *H*, km	**Magnitude** M_w	**Earthquake source length**(i) *L*, km	**Earthquake epicentral distance to wells** d_e, km	d_e/L	**Specific density of seismic energy** *e*, J/m^3	**Earthquake intensity on the MSK-64 scale**(ii)	**Wells (precursor duration, T_1 / precursor lead time T_2**(iiiii)**, weeks)**
1	06.10.1987	52.86ºN 160.23ºE	33	6.5	37	130–134	3.5–3.7	0.1	5	GK-1 (30/30), M-1 (4/4), E-1(iii)(5/5)
2	02.03.1992	52.76ºN 160.20ºE	20	6.9	56	133–136	2.4	0.2	5–6	GK-1 (39/39), M-1 (4/4), E-1(iii)(9.5/9.5)
3	08.06.1993	51.20ºN 157.80ºE	40	7.5	103	220–233	2.1–2.3	0.3	5	GK-1 (4/4), M-1 (4/21.5), E-1(iii)(36/36)
4	13.11.1993	51.79ºN 158.83ºE	40	7.0	62	157–167	2.5–2.7	0.1–0.2	5–6	GK-1 (4/4), M-1 (4/17), E-1(iii)(12/12)
5	01.01.1996	53.88ºN 159.44ºE	0	6.6	41	95–108	2.3–2.6	0.1–0.2	4–5	GK-1 (30/30), M-1 (4/13), G-1 (21.5/21.5)
6	05.12.1997	54.64ºN 162.55ºE	10	7.8	139	305–314	2.2-2.3	0.3–0.4	5–6	GK-1 (21.5/21.5), G-1 (13/13), E-1(iiii)(3/3), YuZ-5(iiii)(3/3)
7	30.01.2016	53.86ºN 158.73ºE	168	7.2	76	70–80	0.9-1.1	2.7–4.1	4	E-1 (3/3), YuZ-5 (15/15)

(i) – maximum linear size of the earthquake source according to (Riznichenko, 1976).
(ii) – Medvedev–Sponheuer–Karnik scale, also known as 12-points MSK-64, is a macroseismic intensity scale used for evaluating the shaking of the Earth's surface based on the observed effects in the earthquake area; the values of points are given for Peropavlovsk-Kamchatsky city.
(iii) – lowering of the water-level with amplitudes >3 cm with at an increased rate (see Table 3 in Kopylova, 2001);
(iiii) – the first description of the precursors in water-level changes within three weeks is given in (Kopylova, 2006);
(iiiii) – precursor duration T_1 – maximum duration of abnormal changes in hydrogeological parameters in the well, precursor lead time T_2 – maximum time from the beginning of an anomalous change in the hydrogeological parameters in the well to the earthquake.

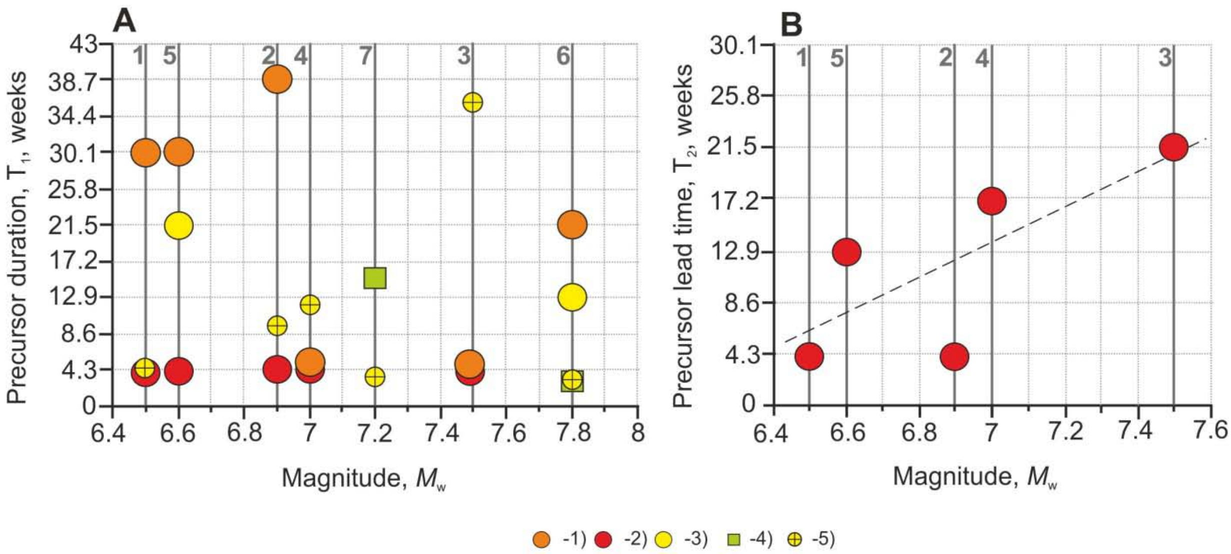

Supplementary Materials Figure S2. A – Distribution of the precursor duration (T_1) in observation wells: 1 – GK-1, 2 – M-1, 3 – G-1, 4 – YuZ-5, 5 – E-1, depending on the magnitude M_w of earthquakes No. 1–7 in **Supplementary Materials Table S2**; earthquakes are shown with gray vertical lines. **B** – Distribution of the lead time (T_2) of hydrogeochemical precursors in the M-1 well (**Supplementary Materials Figure S3B**), depending on the magnitude M_w of earthquakes No. 1–5 (the linear correlation coefficient is 0.74).

Note 1: Hydrogeological precursors of earthquakes No. 1–6 in wells GK-1, M-1, E-1, G-1 are previously presented in (Kopylova et al., 1994, Figures 3,5,7; Kopylova, 2001, Figures 2,8, Table 3; Khatkevich and Ryabinin, 2004, Figures 5,6,7; Kopylova, 2006, Figure 7; Serafimova and Kopylova, 2010, Figure 2; Kopylova and Boldina, 2019, Figure 4), as well as in **Supplementary Materials Figure S3**. Hydrogeological precursors of earthquake No. 7 in water-level changes in wells E-1 and YuZ-5 are previously presented in (Boldina and Kopylova, 2017, Figures 3,9; Kopylova and Boldina, 2019, Figures 7,8), as well as in **Supplementary Materials Figure S5,6**.

Note 2: We believe that the increased duration of hydrogeodynamic precursors in water-level in the E-1 well before earthquakes No. 3 and No. 4 (**Supplementary Materials Table S2)** caused by the superposition of the precursor signals PS1 and PS2 due to the impossibility of correct separation of two signals according to rare and rough observational data in 1987–1994 (Kopylova, 2001).

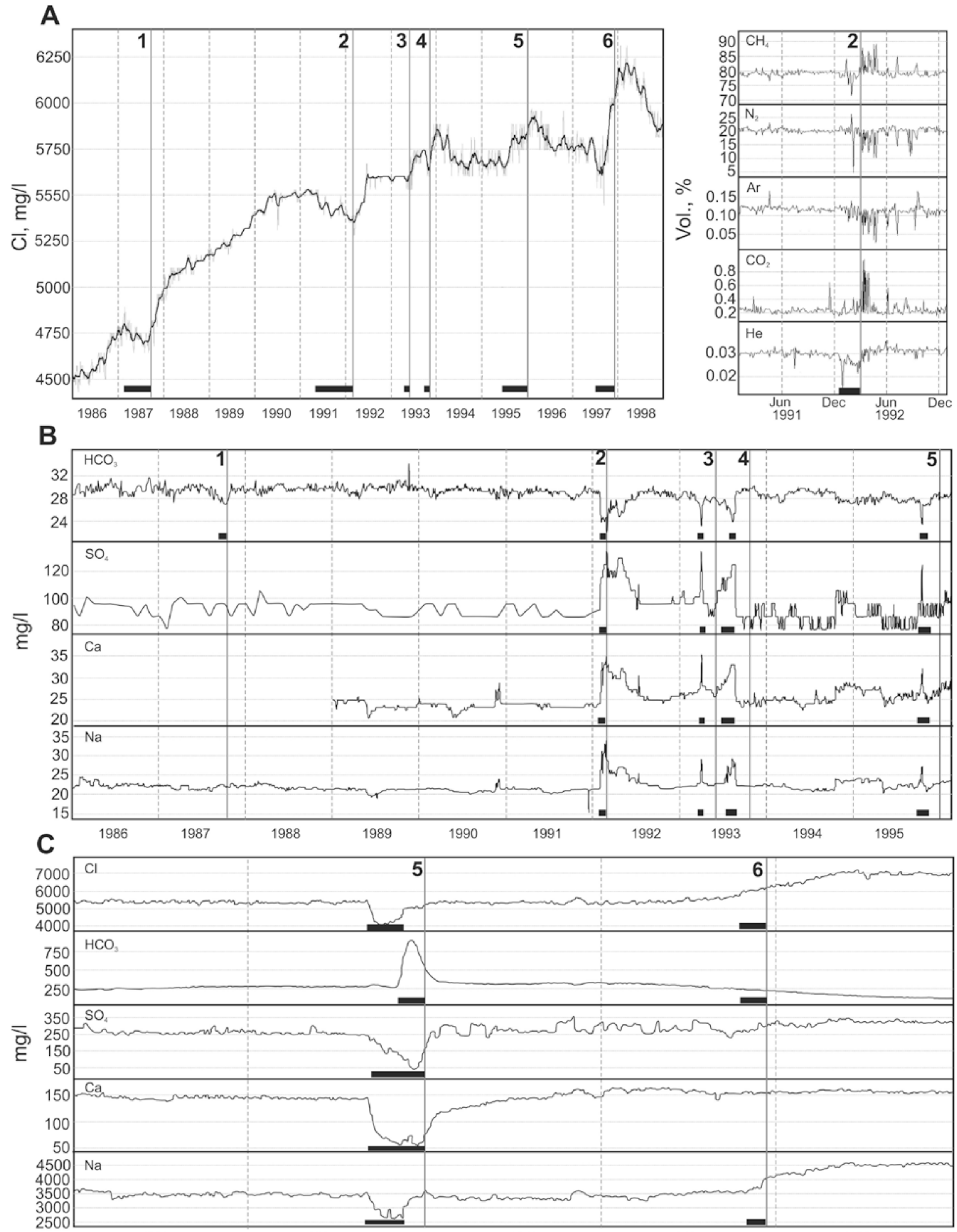

Supplementary Materials Figure S3. Anomalous effects (bold horizontal lines) in the time series of hydrogeochemical parameters of groundwater from flowing wells: **(A)** GK-1, **(B)** M-1, **(C)** G-1. The vertical lines show earthquakes 1987–1997 (**Figure 1A)**, earthquake numbers correspond to the **Supplementary Materials Table S2**.

The Zhupanovsky earthquake of January 30, 2016, M_w=7.2
(No. 7 in **Supplementary Materials Table S2**), E-1 well

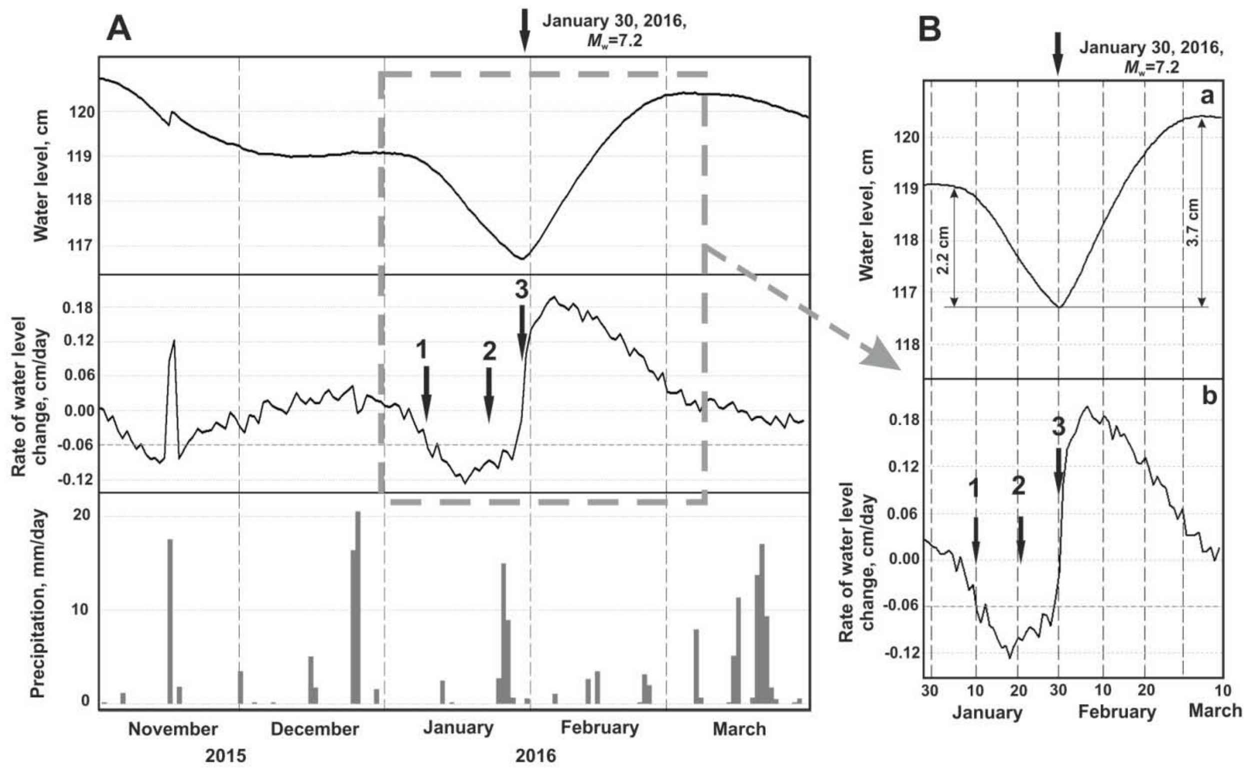

Supplementary Materials Figure S4. Water-level changes in E-1 well:
(A) time series of water-level changes and their average daily rate as compared to time behavior of precipitation, November 2015 to March 2016; the Zhupanovsky earthquake of January 30, 2016, M_w=7.2 is indicated by arrow. Figures on the graph of daily rate of water-level changes: **1,** January 10, the beginning of PS1; **2,** January 21, the date of submission of the prognostic conclusions as to the possibility of strong earthquake to KB REC; **3,** January 30, the Zhupanovsky earthquake. The thin dashed line shows the threshold value of the rate of water-level decrease – -0.06 cm/day. The thick dashed line delineates the fragment of water-level variations shown in Figure **(B)**: (**a)** water-level changes from December 30, 2015 to March 10, 2016 including the manifestation of PS1 and post-seismic increase; (**b)** the change in the average daily rate of water-level variations as compared to the threshold value – -0.06 cm/day (Boldina and Kopylova, 2017).

The Zhupanovsky earthquake of January 30, 2016, M_w=7.2
(No. 7 in **Supplementary Materials Table S2**), YuZ-5 well

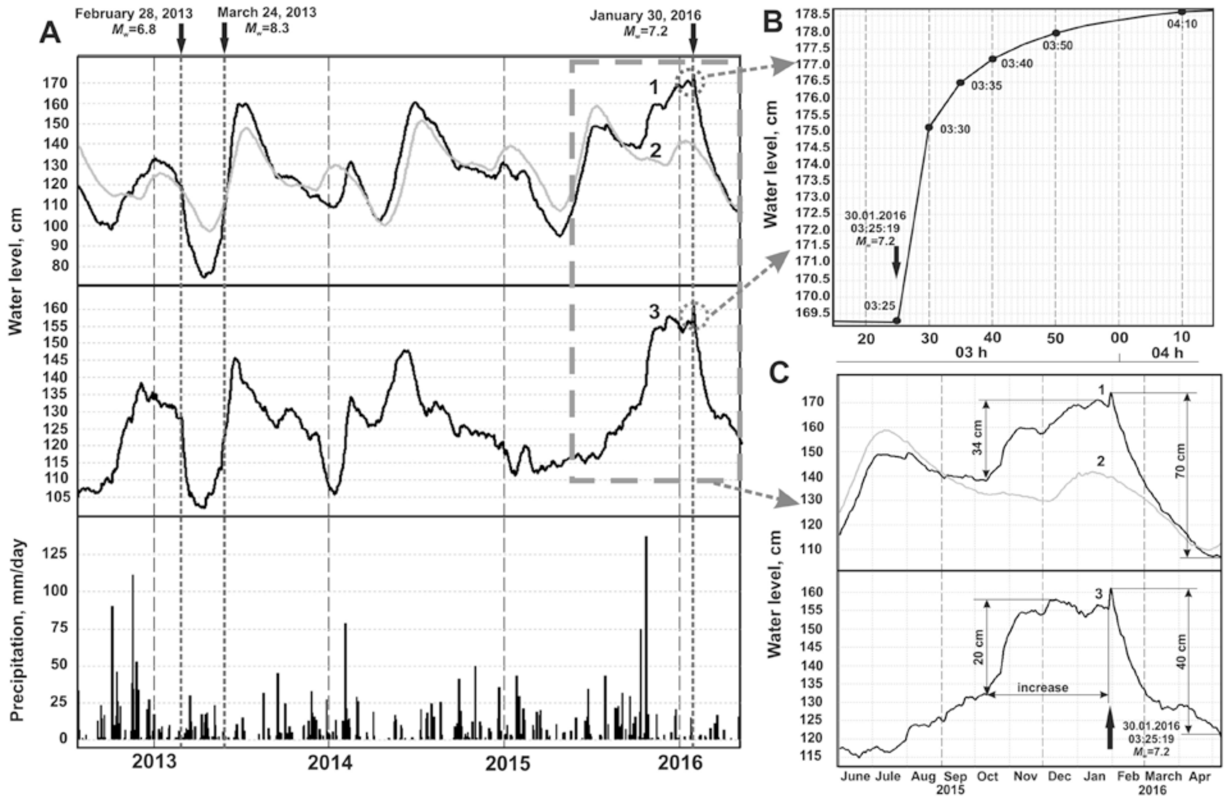

Supplementary Materials Figure S5. Water-level changes in YuZ-5 well:
(A) water-level changes in July 2012 to May 2016 as compared to the time behavior of precipitation and occurrence of earthquakes with $M_w \geq 6.8$ (shown by arrows): 1, average hourly observation data with corrected for baric variations (black line); 2, annual seasonal variations in water-level (gray line); 3, residuals in water-level changes after correction for annual seasonality and trend: bold dashed line indicates a fragment of graphs during the Zhupanovsky earthquake; **(B)** coseismic step in the water-level behavior after the arrival of seismic waves (03:25 UT); **(C)** pre-seismic rise and post-seismic fall in the water-level (Boldina and Kopylova, 2017).

EQ of February 28, 2013, 50.83° N, 157.93° E, M_w=6.8, H=45 km, d_e=270 km **(Figure 1A),**
E-1 well

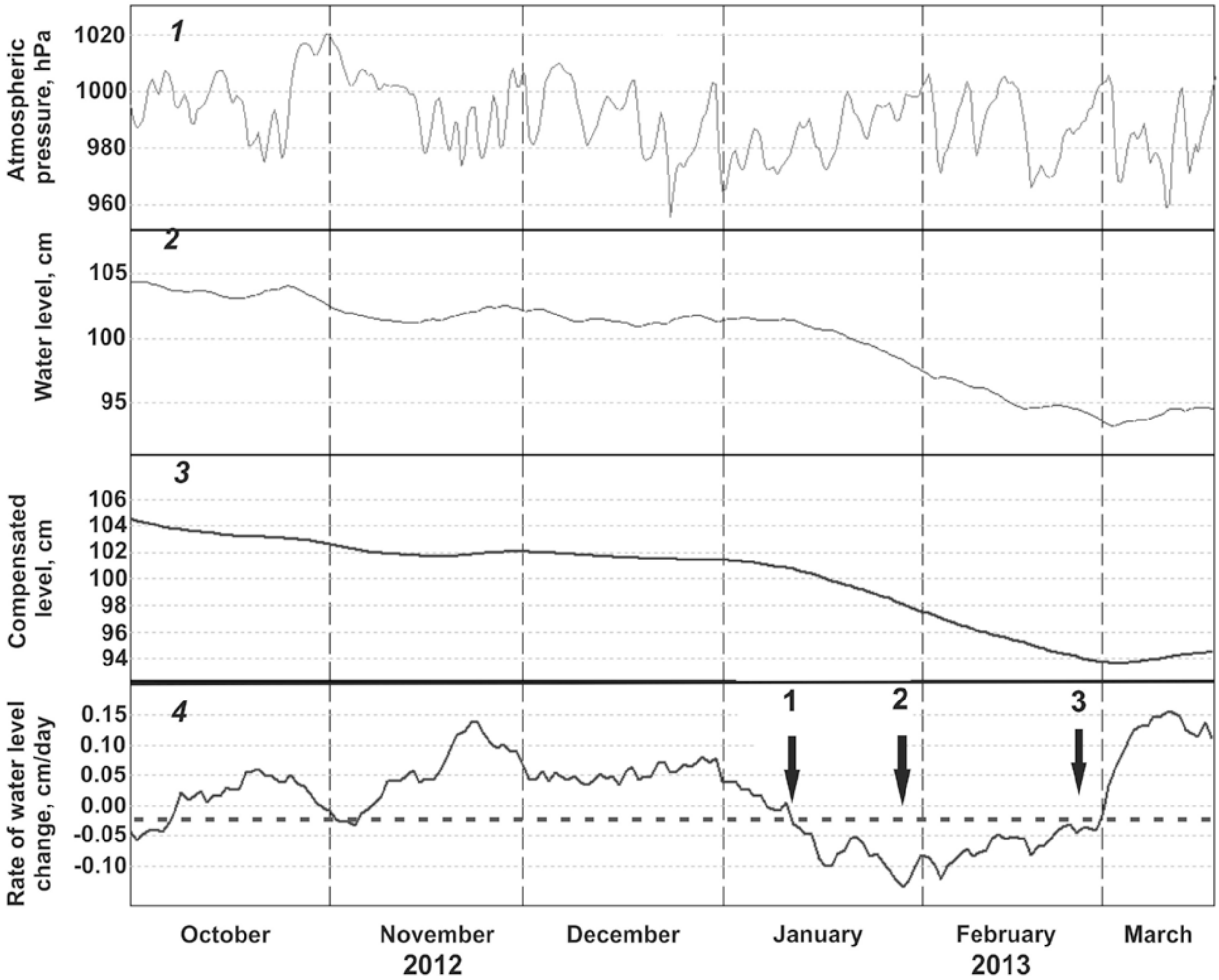

Supplementary Materials Figure S6. Water-level changes in well E-1, October 1, 2012 to March 18, 2013: ***1, 2,*** atmospheric pressure and water-level time series with a sampling interval of 5 min; ***3,*** daily average water-level changes with corrected for baric variations; ***4,*** daily rate of water-level variations: arrows on the graph indicate (**1**) January 16, 2013, the beginning of PS1; (**2**) February 1, 2013, the prognostic conclusions were sent to KB REC (**Supplementary Materials Figure S7)**; (**3**) February 28, 2013, the date of the earthquake. Horizontal dashed line shows the threshold value for the daily rate of water-level variations (Kopylova et al., 2017).

PS1 and PS2 manifestations in water-level changes in E-1 well,
November 2011 to September 2016

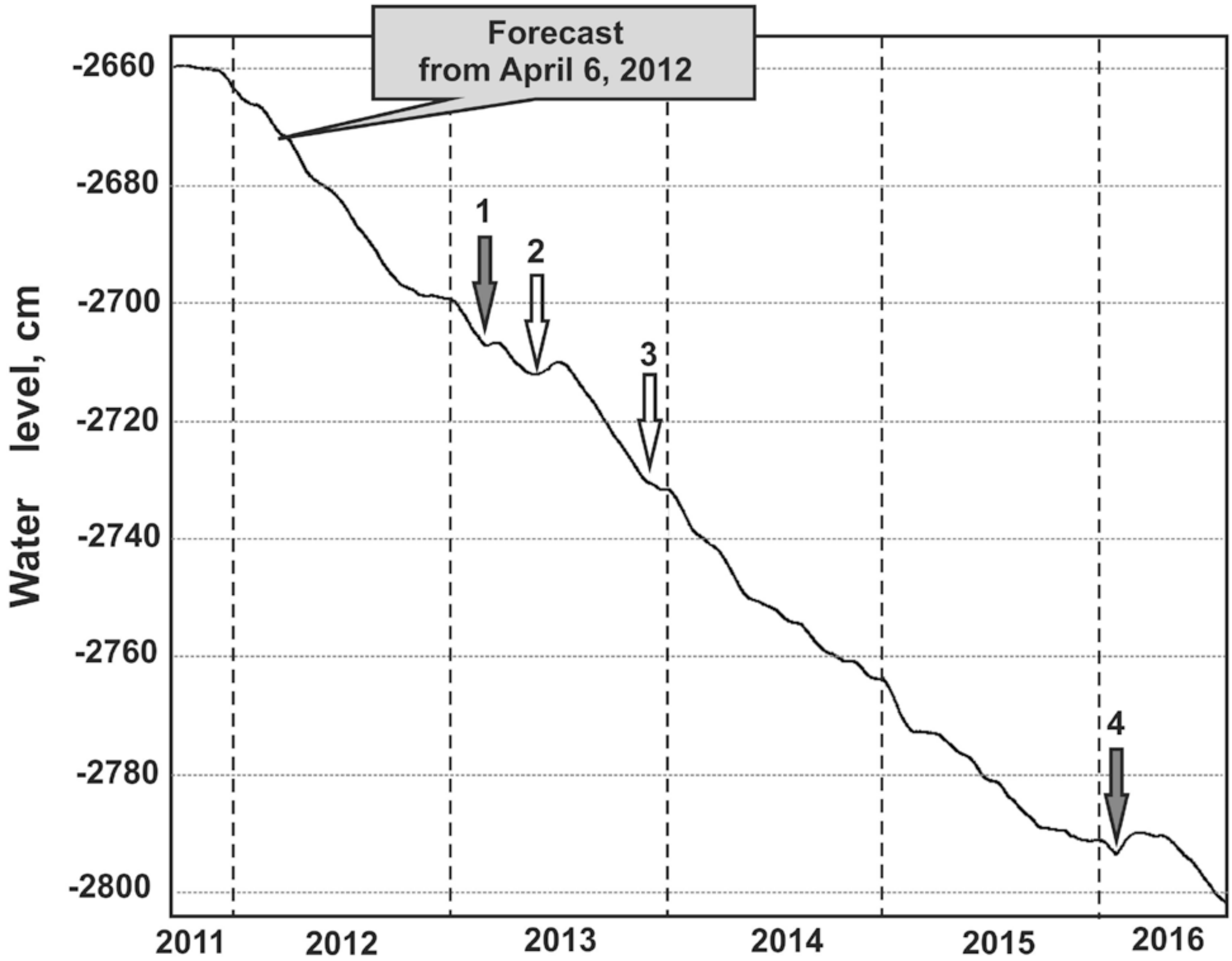

Supplementary Materials Figure S7. The fall in the water-level at increased rate in December 2011 to March 2012, exceeding the maximum duration of PS1, and a similar water-level decrease in 1991–1997 preceding and accompanying the group of strong earthquakes in 1992–1997 (M_{max}=7.8) (Kopylova, 2001) served as the basis for submitting the prognostic conclusion on April 6, 2012 to KB REC. In the conclusion, it was reported that one or more earthquakes with $M_w \geq 6.0$ are probable within a radius of up to first hundreds of kilometers from the well during the months to the first years. This predictive conclusion was based on PS2.

During 2013–2016, more than 20 events with $M_w \geq 6$ took place within a radius of 350 km from the well, most of which were aftershocks of the four major earthquakes with magnitudes M_w=6.6–8.3 (shown by arrows) (Sil'nye.., 2014; Chebrov et al., 2016).

During the development of the long-term water-level lowering, two successful predictions of the main events based on PS1 were made (shown by dark arrows): **1,** February 28, 2013, M_w=6.8 (**Supplementary Materials Figure S6,8)**, **4,** January 30, 2016, M_w=7.2 **Supplementary Materials Figure S4).** Open arrows indicate major earthquakes for which no predictions based on PS1 have been issued: **2**, May 24, 2013, M_w=8.3; **3**, November 12, 2013, M_w=6.6. We believe that the lack of forecasts of these two events is associated with a weak manifestation of PS1 against the background of a long-term water-level lowering and post-seismic water-level variations after the earthquake of February 28, 2013 (**1**) (Firstov et al., 2016; Kopylova et al., 2018).

Supplementary Materials Table S3. Retrospective parametric description of the precursor signal PS1 in water-level changes in the E-1 well
(Kopylova, Sizova, 2012; Kopylova et al., 2019)

Data for analysis	Water-level observation data from well E-1 (53.26°N, 158.48°E), February1996 to October 2012, total observation time **T**=4042 days (10.4 years)
Earthquake monitoring area	A region within a radius of 350 km from the E-1 well
Studied parameter	Daily rate of water-level changes with corrected for baric variations and trend
Precursor signal PS1	The increase in the daily rate of water-level decline to 0.05–0.07 cm/day for at least 5 days
Retrospective analysis of PS1 for forecasting the earthquakes with M≥5.0	
Total number of earthquakes, **n**	59
Total number of PS1 manifestations before earthquakes (successful forecasts), **m**	27
Probability of correlation between PS1 manifestations and earthquakes, **P=m/n**	**P=27/59=0.46**
Probability of missing a target, $\mathbf{P_{mt}}$**=(n–m)/n**	$\mathbf{P_{mt}}$**=(59–27)/59=0.54**
Total number of PS1 manifestations, **m′**	32
Total number of cases when no earthquake occurred after PS1 manifestations (false alarms)	6
Probability of a successful forecasts for PS1 manifestations, **P′=m/m′**	**P′=27/32=0.84**
Probability of false alarm, $\mathbf{P_{fa}}$**=(m′–m)/ m′**	$\mathbf{P_{fa}}$**=(32–27)/32=0.16**
Total alarm time, **τ**	1316 days
Ratio of total alarm time to total observation time, **τ/T**	1316/4042 = 0.33
Efficiency of PS1 for forecasting the earthquakes with magnitude M ≥5.0, **J=P/(τ/T)**	**J=0.46/0.33=1.4**
Retrospective analysis of PS1 for forecasting earthquakes with M_w≥5.8	
Total number of earthquakes, **n**	14
Total number of PS1 manifestations before earthquakes (successful forecasts), **m**	11
Probability of correlation between PS1 manifestations and earthquakes, **P=m/n**	**P=11/14=0.79**
Probability of missing a target, $\mathbf{P_{mt}}$**=(n–m)/n**	$\mathbf{P_{mt}}$**=(14–11)/14=0.21**
Probability of a successful forecast for PS1 manifestations, **P′=m/m′**	**P′=11/32=0.34**
Probability of false alarm, $\mathbf{P_{fa}}$**=(m′–m)/m′**	$\mathbf{P_{fa}}$**=(32–11)/32=0.66**
Efficiency of PS1 for forecasting the earthquakes with magnitude M_w≥5.8, **J=P/(τ/T)**	**J=0.79/0.33=2.4**

Explanation to **Supplementary Materials Table S3.**

A retrospective parametric description of the PS1 precursor signal includes an assessment of five statistical quantities characterizing the features of the relation between the forecasts based on this kind of precursor and subsequent earthquakes of a given energy range and from a given spatial area:

1 **–** probability of a connection between successful forecasts of earthquakes according to PS1 and earthquakes, equal to the ratio of successful forecasts to the total number of earthquakes that have occurred (**P**)**;**

2 **–** probability of missing a target, equal to the ratio of the number of not predicted earthquakes to the total number of earthquakes that occurred ($\mathbf{P_{mt}}$);

3 **–** probability of a successful forecasts of earthquakes during occurrence of PS1, equal to the ratio of the number of PS manifestations before earthquakes to the total number of PS1 manifestations (**P′**);

4 **–** probability of false alarm, equal to the ratio of the number of PS1 manifestations, after which no earthquake occurred, to the total number of PS1 manifestations ($\mathbf{P_{fa}}$);

5 **–** retrospective efficiency of earthquake forecasts on base of PS1 (**J**).

We used the approach (Gusev, 1974) to assess the retrospective efficiency of earthquake forecasts on base of PS1. If the forecast according to the specified technique is given for the same spatial area (within a radius of up to 350 km from well E-1) and for the same energy range of earthquakes ($M \geq 5.0$ and $M_w \geq 5.8$), then the efficiency of this technique **J** can be estimate by the formula

$$\mathbf{J=(m/n)/(\tau/T)=P/(\tau/T)},$$

where **m** is the number of “predicted” earthquakes, that is, those that correspond to successful forecasts; **n** is the total number of earthquakes that occurred with parameters (location–energy) that correspond to the forecast, that is, earthquakes that could be predicted; $\boldsymbol{\tau}$ is total alarm time, that is, the total duration of all successful and unsuccessful forecasts, including the time of all cases of PS1 manifestation up to the moment of the earthquake minus 5 days in each case of PS1 manifestation or, in the case of "false alarms", the durations of PS1 minus 5 days and plus 30 days corresponding to the waiting time of the earthquake after the end of the PS1 manifestation; and **T** is the total time of monitoring the seismic situation by the technique that is being assessed.

Accordingly, the efficiency **J** is the ratio between the number of predicted earthquakes according to PS1 and the number of those events that could occur accidentally during an alarm time, assessed by the ratio of $\boldsymbol{\tau}$**/T**. Obviously, the random guess method would make **J** equal to 1. If the value **J**>1, then this technique is useful for predicting earthquakes.

When drawing up forecast conclusions for the Expert Council on Earthquake Forecasting (**Supplementary Materials Figure S8**), we include information on retrospective statistical assessments of the relationship between the PS1 precursor and subsequent earthquakes, so that the experts of Council have objective data on the significance of the precursor we are using.

In addition to the retrospective statistical assessments, constantly updated empirical data on the duration and lead time of the precursor signal PS1 before earthquakes, as well as estimates of the spatial area of earthquakes, before which PS1 appears, are important in drawing up forecast conclusions. Such empirical evidences are also taken into account in determining the formulation of forecasting conclusions. In particular, for the preparation of forecast statements, the following empirical data on PS1 (average value (range of variations)) are taken into account:

– epicentral distances of earthquakes ($M \geq 5$), which were preceded by the PS1: (80–360) km;

– time of PS1 manifestation: 43 (8–70) days;

– time from the beginning of PS1 to earthquakes with $M \geq 5.0$: 65 (45–105) days.

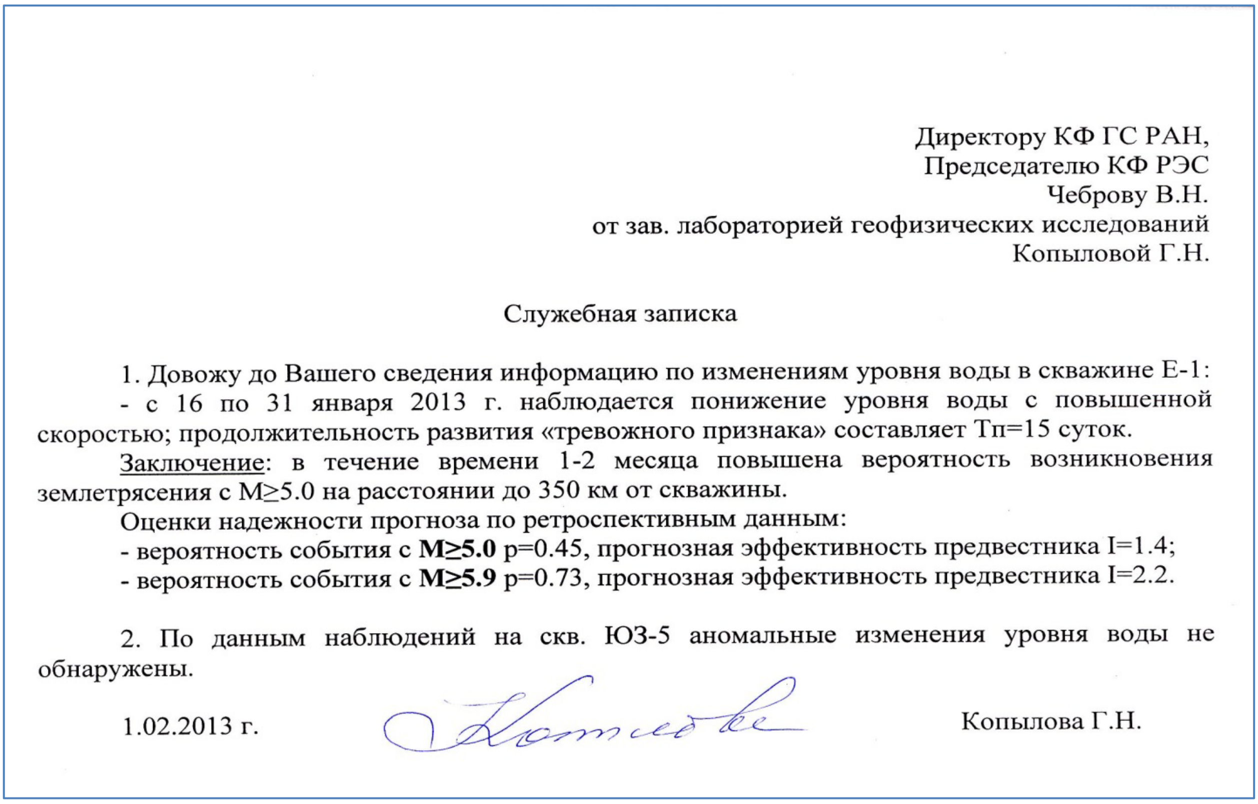

Директору КФ ГС РАН,
Председателю КФ РЭС
Чеброву В.Н.
от зав. лабораторией геофизических исследований
Копыловой Г.Н.

Служебная записка

1. Довожу до Вашего сведения информацию по изменениям уровня воды в скважине Е-1:

- с 16 по 31 января 2013 г. наблюдается понижение уровня воды с повышенной скоростью; продолжительность развития «тревожного признака» составляет Тп=15 суток.

<u>Заключение</u>: в течение времени 1-2 месяца повышена вероятность возникновения землетрясения с М≥5.0 на расстоянии до 350 км от скважины.

Оценки надежности прогноза по ретроспективным данным:

- вероятность события с **М≥5.0** p=0.45, прогнозная эффективность предвестника I=1.4;
- вероятность события с **М≥5.9** p=0.73, прогнозная эффективность предвестника I=2.2.

2. По данным наблюдений на скв. ЮЗ-5 аномальные изменения уровня воды не обнаружены.

1.02.2013 г. Копылова Г.Н.

Supplementary Materials Figure S8. An example of a forecast report dated February 1, 2013, submitted to the Kamchatka branch of the Russian Expert Council for Earthquake Forecast, Seismic Hazard and Risk Assessment (KB REC). The **Supplementary Materials Figure S6** presents the observation data from E-1 well**.** In the **Supplementary Materials Table S3,** retrospective estimates of the precursor PS1 efficiency for forecasting earthquakes with $M \geq 5.0$ and $M_w \geq 5.8$ are presented.

Translation

To Director of KB GS RAS,
Head of the KB REC
Chebrov V.N.
From Head of laboratory of geophysical research
Kopylova G.N.

1. Bring to your attention information on water-level changes in E-1 well:

– from January 16 to January 31, 2013, water-level decreases at higher rate; the duration of the “warning signal” is T=15 days.

<u>Conclusions</u>: over a period of 1–2 months, there is an increased probability of an earthquake with $M \geq 5.0$ to occur at a distance up to 350 km from the well.

The forecast reliability estimates based on the retrospective data are following:

– probability of the event with $M \geq 5.0$ is P=0.45, the prognostic efficiency of the precursor is J=1.4;

– probability of the event with $M \geq 5.9$ is P=0.73, the prognostic efficiency of the precursor is J=2.2.

2. In the observations at YuZ-5 well, anomalous water-level changes are not detected.

February 1, 2013 Kopylova G.N.

Referenses

Chebrov, V. N., Kugayenko, Yu. A., Abubakirov, I. R., Droznina, S. Ya., Ivanova, Ye. I., Matveyenko, Ye.A., et al. (2016). The January 30th, 2016 earthquake with K_s=15.7, M_w=7.2, I=6 in the Zhupanovsky region (Kamchatka). *Vestnik KRAUNTS. Seriya Nauki o Zemle.* 29(1), 5–16. (in Russian).
http://www.kscnet.ru/journal/kraesc/article/viewFile/65/pdf

Kopylova, G. N., Boldina, S. V., and Chubarova, E. G. (2018). “Water-level changes in the well E-1 as an indicator of geodynamic conditions in Koryaksky-Avachinsky volcano-tectonic depression, Kamchatka” in Proceedings 2nd Geothermal Volcanology Workshop (Petropavlovsk-Kamchatsky: Institute of Volcanology and Seismology FEB RAS), 33–37. (in Russian).
http://www.kscnet.ru/ivs/conferences/documents/proceedings.pdf

Kopylova, G. N., Boldina, S. V., and Polyakov, A. Y. (2019). “Hydrogeodynamic Precursors of Earthquakes According to Observations in the Wells of the Petropavlovsk Geodynamic Polygon and Mutnovsky Geothermal Field, Kamchatka Peninsula, Russia” in Proceedings 3nd Geothermal Volcanology Workshop (Petropavlovsk-Kamchatsky: Institute of Volcanology and Seismology FEB RAS), 51–55. (in Russian).
http://www.kscnet.ru/ivs/conferences/GeothermVolc2019/PROCEEDINGS-2019.pdf

Kopylova, G. N., and Sizova, Ye. G. (2012). “On the precursor of earthquakes, manifested in changes of the water-level in the E-1 well, Kamchatka” in Proceedings of the regional conference Volcanism and related processes, dedicated Volcanologist's Day, 29-30 March 2012 (Petropavlovsk-Kamchatsky: Institute of Volcanology and Seismology FEB RAS), 116–125. (in Russian).
http://www.kscnet.ru/ivs/publication/volc_day/2012/art19.pdf

Sil’nye kamchatskie zemletryaseniya 2013 goda (Strong Earthquakes of Kamchatka in 2013). (2014). Ed. V. N. Chebrov (Petropavlovsk-Kamchatsky: Novaya kniga). (in Russian).
http://emsd.ru/static/library/2014_eqkam/book.pdf

Firstov, P. P., Kopylova, G. N., Solomatin, A. V., and Serafimova, Yu. K. (2016). Strong earthquakes forecast near the Kamchatka peninsula. *Vestnik KRAUNTS. Seriya Nauki o Zemle.* 32(4), 106–114. (in Russian).
http://www.kscnet.ru/journal/kraesc/article/viewFile/106/pdf